

# PROOF-OF-PRINCIPLE TESTS FOR SLIT-SCAN-BASED SLICE EMITTANCE MEASUREMENTS AT PITZ

R. Niemczyk\*, H. Huck<sup>†</sup>, P. Boonpornprasert, Y. Chen, J. Good, M. Gross, I. Isaev, D. Kalantaryan, C. Koschitzki, M. Krasilnikov, X. Li, O. Lishilin, G. Loisch, D. Melkumyan, A. Oppelt, H. Qian, Y. Renier, C. Saisa-ard<sup>‡</sup>, F. Stephan, Q. Zhao<sup>§</sup>, DESY, 15738 Zeuthen, Germany  
W. Hillert, University Hamburg, 22761 Hamburg, Germany

## Abstract

Transverse slice emittance is one of the most important properties of high-brightness electron beams for free-electron lasers (FELs). The photo injector test facility at DESY in Zeuthen (PITZ) develops high-brightness electron sources for modern FELs. With a 23 MeV, 1 nC beam at PITZ the experimental slice emittance characterization with the quadrupole scan technique is complicated by strong space charge effects. Combining the slit scan technique with a transverse deflecting cavity (TDS) allows for time-resolved emittance measurements of such a space-charge-dominated beam. The first proof-of-principle results of slice emittance measurements at PITZ based on the 'TDS + slit scan'-technique are presented in this paper.

## INTRODUCTION

At the Photo Injector Test facility at DESY in Zeuthen (PITZ) electron guns are developed and optimized for superconducting LINAC-based free-electron lasers (FELs) like FLASH and the European XFEL [1]. Besides gun development, plasma wakefield acceleration (PWFA) [2], accelerator-based THz generation [3] and electron diffraction [4] are also investigated at PITZ.

For FELs, emittance is one of the key parameters for the gain length [5]. Here, the properties of the central slices, i.e., the slices with the highest charges are important, since these slices will rather contribute to lasing than the low-charged head and tail of the bunch [6]. This motivates optimization of the photoinjector not only for projected, but also for slice emittance, especially since simulation results show that the optimum photoinjector setting for both might be different [7]. While a satisfying technique to measure slice emittance at intermediate electron energies exists [6], measurements of the slice emittance at low energies are heavily complicated by space charge forces. These lead to a deviation between the

actual beam transport and the beam transport suggested by algorithms [7]. At PITZ, the standard technique to measure the projected emittance is the slit scan [8–10]. The information of the transverse slit position, together with the beamlet size, allows to reconstruct the transverse phase space, so that the normalized emittance can be calculated via

$$\epsilon_{n,x} = \beta\gamma\sqrt{\langle x^2 \rangle \langle x'^2 \rangle - \langle xx' \rangle^2}, \quad (1)$$

where  $\beta = v/c$ , with  $v$  the electron velocity,  $c$  the speed of light,  $\gamma$  the Lorentz factor and  $\langle x^2 \rangle$ ,  $\langle x'^2 \rangle$  and  $\langle xx' \rangle$  the second-order beam moments. Employing an rf deflector (TDS) allows the measurement of the slice emittance. High-charge beams with low momenta are observed at photoinjector test facilities and energy recovery LINACs [11, 12], opening the demand for space-charge-resistive slice emittance diagnostics.

## MEASUREMENT SET-UP

An overview of the PITZ beamline is given in Fig. 1. The electrons are generated with an UV laser at a  $\text{Cs}_2\text{Te}$  photocathode inside the rf gun, which accelerates the electrons to  $\sim 6$  MeV. Up to 600 electron bunches are generated with a spacing of  $1\ \mu\text{s}$  inside a bunch train and a bunch train repetition rate of 10 Hz [1]. A booster further accelerates the electrons to an energy of  $\sim 23$  MeV. A normalized emittance of the electron beam down to  $0.7\ \mu\text{m}$  for bunches with 1 nC has been obtained [1].

The PITZ beamline is equipped with three emittance measurement system (EMSY) stations, at which a slit mask is located. The mask has slits with  $10\ \mu\text{m}$  and  $50\ \mu\text{m}$  opening, while only the  $10\ \mu\text{m}$ -wide slit is used for measurement of the projected emittance at high charge [13]. During the here presented measurement the  $50\ \mu\text{m}$ -wide slit has been used to get a high signal-to-noise ration for the streaked beam. Two EMSY stations are located upstream the TDS, while the third one is upstream the dispersive section HEDA2. For the first slice emittance measurements the second EMSY station has been chosen as slit position to minimize the distance

\* raffael.niemczyk@desy.de

<sup>†</sup> holger.huck@desy.de

<sup>‡</sup> On leave from Chiang Mai University, Chiang Mai, Thailand

<sup>§</sup> On leave from IMP/CAS, Lanzhou, China

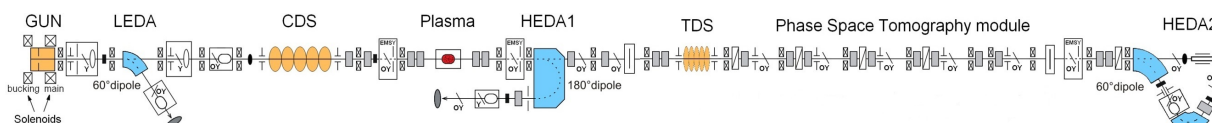


Figure 1: Schematic of the PITZ beamline. The electrons travel from left to right. The plasma cell was not mounted during the slice emittance measurement.

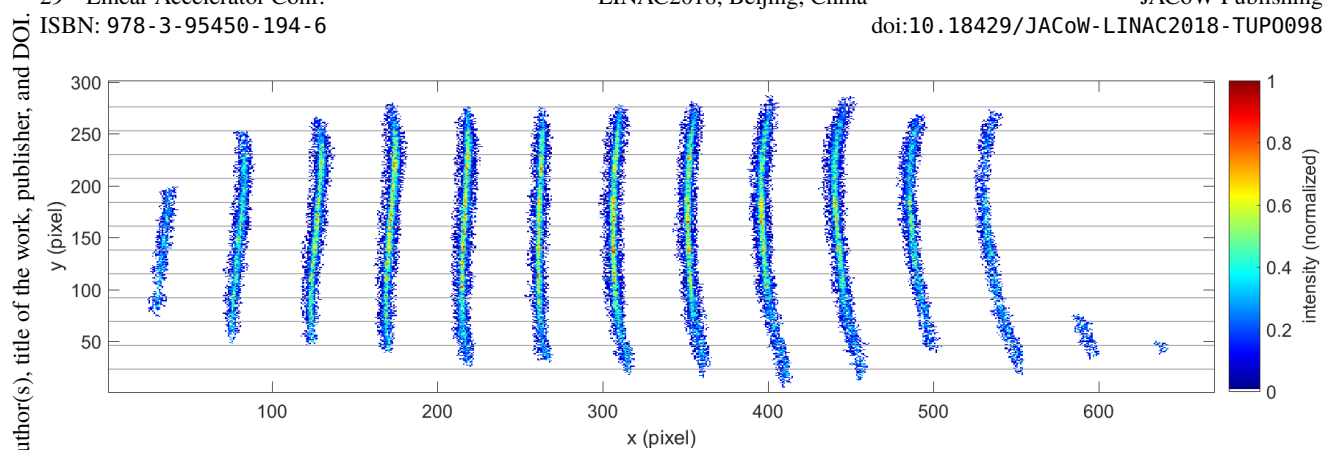


Figure 2: Streaked beamlet images on the observation screen after noise cut. The streak is in the vertical direction  $y$ , hence the beamlet images are sliced in the vertical plane. From the horizontal profile of each slice the phase space is reconstructed. The beamlet images have been shifted horizontally to not overlap.

Table 1: Longitudinal Position of Devices at the PITZ Beamline

Element	Long. Position (m)
Cathode surface	0
EMSY1	5.277
EMSY2	7.125
TDS centre	10.985
Observation screen	12.278
EMSY3	16.303

to the TDS where space charge forces act on the beamlet, see Table 1. The TDS streaks the electrons in the vertical plane to measure the slice emittance in the horizontal plane [7]. It has been developed by the Institute for Nuclear Research (INR RAS, Moscow, Russia) in collaboration with DESY [14]. The repetition rate of the TDS is 10 Hz, while the maximum rf pulse length is 3  $\mu$ s, allowing to streak three consecutive electron bunches from each bunch train, i.e., sum up the signal from three bunches on each image. As observation screen, the first screen downstream the TDS has been chosen, an ytterbium aluminium garnet powder (YAG) screen.

The slice emittance measurement has been carried out with a bunch charge of 500 pC. The laser pulse had  $\sim$ 11 ps FWHM pulse length and a roughly Gaussian time profile. The estimated cathode gradient was 58.2 MV/m, the gun and booster phases were set for maximum acceleration. The FWHM electron bunch length was  $(14.1 \pm 0.5)$  ps, measured with the TDS with a time resolution of 0.8 ps. For the slice emittance measurement presented here, 14 slit positions with 300  $\mu$ m spacing have been used. Only a small number of slit positions was used since the data acquisition was not automated yet.

## RESULTS

Images of the streaked beamlets are given in Fig. 2. When projected onto the horizontal axis  $x$ , the phase space of the

projected beam as well as the projected emittance can be calculated.

### Projected Emittance

The phase space of the projected distribution is given in Fig. 3. The beam size obtained from the beamlet images  $\sqrt{\langle x^2 \rangle}$  is typically smaller than the beam size  $\sigma_x$  measured with a scintillator screen at the slit position due to lower intensity at the outer slit positions. To account for this fact, at PITZ the scaled emittance

$$\epsilon_{n,x,\text{scaled}} = \frac{\sigma_x}{\sqrt{\langle x^2 \rangle}} \epsilon_{n,x} \quad (2)$$

is used [1]. The unscaled, normalized emittance in the horizontal plane was measured to be 1.3  $\mu$ m, while the scaled, normalized emittance was 2.3  $\mu$ m. However, the unscaled projected emittance was measured to be 1.9  $\mu$ m with the standard software. Besides the switched-off TDS, both methods differ in a different noise cut and the number of slit positions.

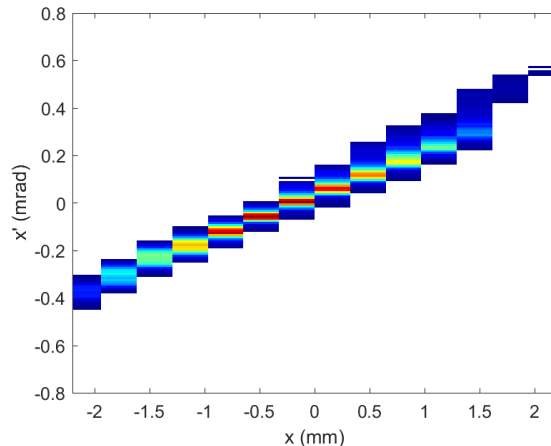


Figure 3: Phase space of the projected electron distribution in the horizontal plane. For the reconstruction of the projected phase space the images of the streaked beamlets have been projected onto the horizontal axis. The scaled, normalized emittance is 2.3  $\mu$ m.

For the slice emittance measurement only 14 slit positions have been used due to missing automation, while approx. 130 slit positions have been used for the measurement of the projected emittance. Additionally, the signal-to-noise ratio is smaller during the slice emittance measurements since the charge is distributed on a larger screen area. The low intensity on the observation screen due to the rf streak and the slit mask, especially at the outer slit positions, lead to a big scaling factor. The measured emittance is much higher than the usually achieved values for this charge at PITZ. This is due to the fact that the photoinjector was not optimized for minimal emittance for this proof-of-principle experiments, e.g., the laser shape was Gaussian and too short in time, while a longitudinal flattop laser profile with  $\sim 21$  ps FWHM yields a smaller emittance. Furthermore, the lowest emittance is measured at EMSY1 [1]. Also, the focussing of the electron beam, as well as the laser beam size on the cathode were not optimized. In addition to the slice emittance, the projected emittance was measured with the standard software while the TDS was off. The measured scaled, projected emittance was  $2.3 \mu\text{m}$  which agrees well with the calculated parameter of the projected emittance from the slice emittance measurement.

### Slice Emittance

The scaled and unscaled emittance along the longitudinal bunch axis is given in Fig. 4. The normalized, unscaled emittance for the centre slice, i.e., slice number 0, is  $0.76 \mu\text{m}$ , while the scaled emittance for this slice is  $1.3 \mu\text{m}$ . The scaling of the slice emittance is done similarly to the scaling of the projected emittance via

$$\epsilon_{i, \text{scaled}} = \frac{\sigma_{x,i}}{\sqrt{\langle x^2 \rangle_i}} \epsilon_{n,x}, \quad (3)$$

where  $\sqrt{\langle x^2 \rangle_i}$  is the beam size of the slice  $i$ , obtained from the beamlet images and  $\sigma_{x,i}$  the beam size of the slice  $i$  at the

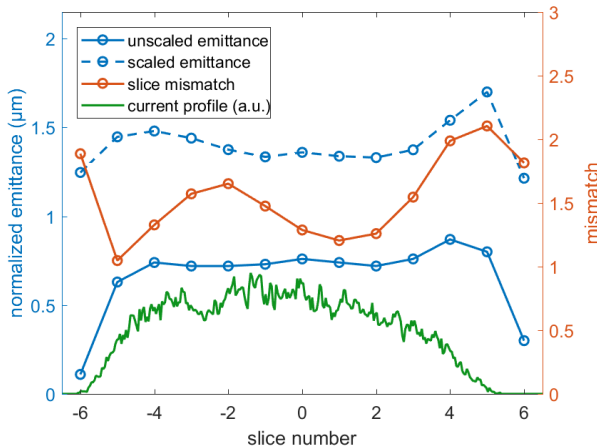


Figure 4: Evolution of the scaled and unscaled emittance along the longitudinal bunch axis, slice mismatch and bunch current profile. The slice emittance is scaled according to Eq. (3), the mismatch is calculated via Eq. (4).

slit position. However, this beam size can not be measured. The slice beam size  $\sigma_{x,i}$  is approximated with  $\sigma_x$  assuming the same initial beam size for all slices. The emittance is almost flat for most of the slices, just at both ends the unscaled emittance drops to smaller values. This is probably due to the low charge at the ends of the almost Gaussian distribution. The lower-charged slices contribute less to the projected emittance than the bunch centre. Moreover, the mismatch of the slices contributes to a higher projected emittance. At PITZ, no specific design optics exists for slice emittance measurements. Therefore, the slice mismatch, shown in Fig. 4, is calculated via

$$M_i = \frac{1}{2} (\beta_i \gamma_P - 2\alpha_i \alpha_P + \gamma_i \beta_P), \quad (4)$$

where  $\alpha_P, \beta_P$  and  $\gamma_P$  are the Twiss parameters of the projected distribution and  $\alpha_i, \beta_i$  and  $\gamma_i$  the Twiss parameters of slice  $i$  correspondingly. The phase space of the centre slice is given in Fig. 5. In comparison to the phase space of the projected bunch a smaller width was measured.

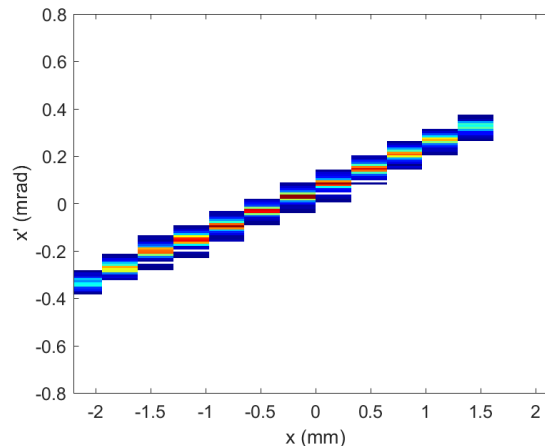


Figure 5: Phase space of the central slice, i.e., slice 0 in Fig. 4, in the horizontal plane. In comparison to the projected phase space, the slice phase space has a smaller width. The scaled, normalized slice emittance is  $1.3 \mu\text{m}$ .

### CONCLUSION

This paper shows the first successful proof-of-principle slice emittance measurement done at PITZ, by means of a single-slit scan and usage of a transverse deflecting cavity (TDS). The scaled central slice emittance was measured to be  $1.3 \mu\text{m}$ , while the unscaled value was  $0.76 \mu\text{m}$ . The scaled, projected emittance, calculated from the streaked beamlets is  $2.3 \mu\text{m}$ . The same value was measured with the unstreaked beam and the standard software at PITZ.

High-intensity screens have been installed to solve low-intensity problems when the beam is streaked [15] and the data taking has been automated. Next steps are the comparison of measurements with different number of slit positions, slit widths, EMSY stations, etc. Then the systematic error of the slice emittance measurement has to be determined before the beam dynamics can be investigated.

## REFERENCES

- [1] M. Krasilnikov *et al.*, “Experimentally minimized beam emittance from an L-band photoinjector”, *Phys. Rev. ST Accel. Beams*, vol. 15, p. 100701, 2012.
- [2] M. Gross *et al.*, “Observation of the Self-Modulation Instability via Time-Resolved Measurements”, *Phys. Rev. Lett.*, vol. 120, p. 144802, 2018.
- [3] P. Boonpornprasert *et al.*, “Calculations for a THz SASE FEL based on the measured Electron Beam Parameters at PITZ”, in *Proc. FEL'17*, Santa Fe, NM, USA, Aug. 2017, pp. 419–421. <https://doi.org/10.18429/JACoW-FEL2017-WEPO04>
- [4] H. Qian *et al.*, “Investigation of High Repetition Rate Femtosecond Electron Diffraction at PITZ”, in *Proc. IPAC'17*, Copenhagen, Denmark, May 2017, p. 3727–3729. <https://doi.org/10.18429/JACoW-IPAC2017-THPAB017>
- [5] E. J. Jaeschke *et al.*, “Synchrotron Light Sources and Free-Electron Lasers”, Springer Reference, p. 155, 2016.
- [6] M. Yan, “Online diagnostics of time-resolved electron beam properties with femtosecond resolution for X-ray FELs”, dissertation, Universität Hamburg, Germany, 2015.
- [7] H. Huck *et al.*, “Progress on the PITZ TDS”, in *Proc. IBIC'16*, Barcelona, Spain, Sep. 2016, pp. 744–747. <https://doi.org/10.18429/JACoW-IBIC2016-WEPG47>
- [8] L. Staykov, “Characterization of the transverse phase space at the photo-injector test facility in DESY, Zeuthen site”, dissertation, Universität Hamburg, Germany, 2008.
- [9] G. Vashchenko, “Transverse phase space studies with the new CDS booster cavity at PITZ”, dissertation, Universität Hamburg, Germany, 2013.
- [10] V. Miltchev, “Investigations on the transverse phase space at a photo injector for minimized emittance”, dissertation, Humboldt-Universität zu Berlin, Germany, 2006.
- [11] J. Baehr, “Low energy high brilliance beam characterization”, in *Proc. DIPAC'05*, Lyon, France, Jun. 2005, paper ITWA01, pp. 307–311.
- [12] L. Merminga, “Energy Recovery LINACs”, in *Proc. PAC'07*, Albuquerque, NM, USA, Jun. 2007, paper MOYKI03, pp. 22–26.
- [13] L. Staykov, “Design Optimization of an Emittance Measurement System at PITZ”, in *Proc. DIPAC'05*, Lyon, France, Jun. 2005, paper POT032, pp. 220–222.
- [14] L. Kravchuk *et al.*, “Layout of the PITZ Transverse Deflecting System for Longitudinal Phase Space and Slice Emittance Measurements”, in *Proc. LINAC'10*, Tsukuba, Japan, Sep. 2010, paper TUP011, p. 416.
- [15] R. Niemczyk *et al.*, “Comparison of YAG screens and LYSO screens at PITZ”, presented at IBIC'18, Shanghai, China, Sep. 2018, paper WEPB04.